PHYSICS CONSIDERATIONS AND SPECIFICATIONS FOR THE NSLS-II MAGNETS *

W. Guo†, S.L. Kramer, S. Krinsky, B. Nash, J. Skaritaka, F. Willeke
BNL, Upton, NY 11973, USA

Abstract

NSLS-II is a third-generation light source that is being built at the Brookhaven National Laboratory. The storage ring has 30 double-bend-achromatic cells. Six 3.5-m-long damping wigglers (DW) will be installed in three straight section to lower the emittance. The civil construction of the facility started in June 2009 and major accelerator components, such as magnets and vacuum chambers, have entered production phase. This paper will summarize the physics considerations for the NSLS-II magnet specifications. In particular, we discuss the tuning range required by the lattice flexibility, and the issues which lead to the specification for the higher-order multipoles.

Table 1: NSLS-II main parameters

Energy (GeV)	3
Circumference (m)	792
Emittance ϵ_x/ϵ_y (nm/pm)	1/8
Chromaticity per cell (x/y)	-3.2/-1.4
Momentum compaction	3.6×10^{-4}
Energy loss 0/6 DWs (MeV)	0.0191/ 0.225
Momentum spread 0/6 DWs ($\times 10^{-4}$)	5.1 / 8.3
Longitudinal damping time 0/6 DWs (ms)	27.7 / 11.8
Harmonic number	1320
RF frequency (MHz)	500
Total current (mA)	500

THE NSLS-II LATTICE AND PARAMETERS

The basic module of the NSLS-II lattice is a standard double-bend-achromatic (DBA) lattice. As shown in Fig. 1 there are three quadrupoles in each of the two matching sections, and two quadrupole doublets in the arc section. There are three sextupole families on each of the three multipole girders, which amounts to nine totally. Some main parameters of NSLS-II are listed in Tab. 1.

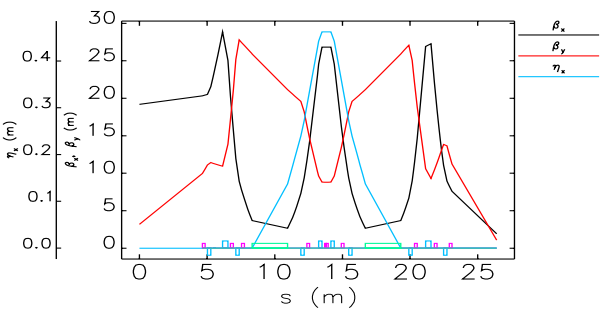

Figure 1: One cell of the NSLS-II DBA lattice. The quadrupole magnets in order are named as: Long straight, QH1, QH2, QH3, QM1, QM2, QM2, QM1, QL3, QL2, QL1, short straight.

LATTICE FLEXIBILITY AND QUADRUPOLE TUNING RANGE

The magnet tuning range is determined from the tune search. It is well known that the betatron phase advances of a Chasman-Green cell are approximately 2π in the horizontal direction and π in the vertical plane. There are 30 cells in our lattice; therefore, we expect the integer part of the tunes to be not far from 30 (H) and 15 (V). The tunes of the present working point are (33.148,16.27). The tunes are on the larger side because the beta functions are focused to small values in the short straight. It would be nice to consider solutions in big ranges; however, we found that if we want to keep small emittance and small β_x ($\sim$3m) in the short straight, the horizontal tune can not be lowered too much. The vertical tune has more flexibility on the lower side. On the upper side both tunes are limited by chromaticity. The chromaticity becomes much greater at larger tunes, which makes the nonlinear optimization and dynamic aperture search difficult. Based on these considerations, we have decided to define the tuning range to be ± 1 units from (33,16). We search for a grid of working points in this tune window. As for the number of points on the grid, we found that the tunes can be varied continuously in a small region and the dynamic aperture is not very sensitive to small tune changes. Consequently we have decided it is adequate to separate the working point by 0.2 units on the grid. And we can always zoom-in on an interesting area if more points are needed. The following constraints are

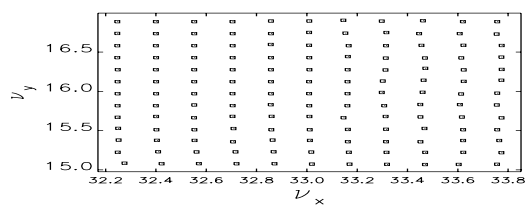

Figure 2: The solutions on a grid of working points.

applied when the lattice is tuned to the other work points:

* Work supported by Brookhaven Science Associates, LLC under Contract No. DE-AC02-98CH10886 with the U.S. Department of Energy.
† wguo@bnl.gov

the natural emittance $\epsilon_x \sim 2$ nm, the natual chromaticities $|\xi_x| < 3.7$ and $|\xi_y| < 1.8$ per DBA, the strict achromatic condition, i.e., the dispersion must be zero in both of the straight sections. The beta functions in the long straight are constrained to $\beta_x \sim 20$ m, $\beta_y \sim 3.5$ m, and in the short straight $\beta_x < 3$ m, $\beta_y \sim 1$ m. And symmetry conditions are kept at the center of the straights and at the arc center between the two dipole magnets. Note that some of the constraints are degenerate. For example, if symmetry condition is imposed at the arc center, then dispersion needs to be constrained only at one exit of the dipole because of the symmetric layout of the quadrupoles. The tunes of the grid of good solutions are shown in Fig. 2.

While working out solutions on the grid, we constrained the beta functions at the straights. However, in some cases different beta functions are desired. In the long straights large β_x is required for injection; however, smaller values are probably preferred if an undulator is put in the long straight. Beta functions in the short straight might be adjusted due to particular requirements from the users, too. Based on these considerations, we have found solutions with different beta functions in straights. Fig. 3 shows solutions with $\beta_x = 13$ and 8 m, and β_y is varied from 1 to 5 m. The tuning range of the quadrupoles can be deduced from these solutions. The statistics of the K_1 values are shown in Tab. 2. We note that the lengths of the quadrupoles have been adjusted recently; however, the integrated strength is kept the same. We found that lowering β_x in the long straight changes the tuning range of QH1 and QH2 significantly. On the other hand, the matching of the insertion devices needs only a small change ($\Delta K_1 < 0.1$); therefore, the listed tuning ranges should cover the required strength change for ID matching.

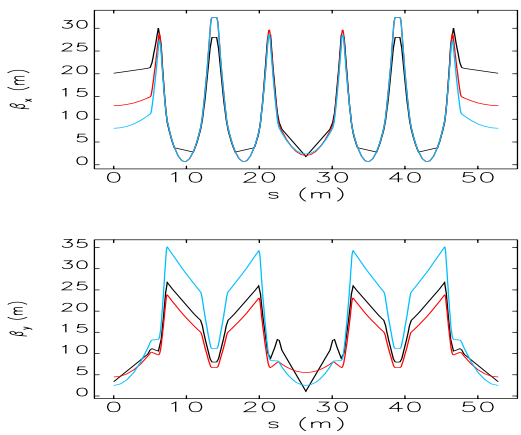

Figure 3: The variation of the beta functions (upper: β_x, lower: β_y) in the straights. The black curves are for the present values.

The tuning ranges for the sextupoles cannot be determined as precisely. The nonlinear solution is usually not unique for a given linear lattice. The tuning range for the three chromatic sextupoles can be deduced from the linear and second-order chromaticity correction. For them the maximum strength is set to $K_{2,max}$=40, which is a conservative number compared to the maximum of ~30 needed for the solutions shown in Fig. 2. Next we found that the maximum strength of the harmonic sextupoles could be set to a value similar to the chromatic sextupole setting. This is understandable because we do not want to introduce extra nonlinearity. We set $K_{2,max}$=40 for all the sextupoles and optimized all the solutions on the grid. So far the optimization is not limited by the maximum strength.

Table 2: The tuning range of the quadrupoles. Units: $1/m^2$ unless specified.

Magnet	L (m)	Nominal	Min.	Max.	σ
QH1	0.25	-0.5095	0.4000	1.7792	0.1689
QH2	0.4	1.5525	1.4755	2.0047	0.0761
QH3	0.25	-1.8238	1.4069	1.9410	0.0636
QL1	0.25	-1.8366	0.7429	2.2000	0.3219
QL2	0.4	2.0079	1.8095	2.0458	0.0447
QL3	0.25	-1.5118	1.2102	1.7561	0.1355
QM1	0.25	-0.8553	0.7295	1.0843	0.0586
QM2	0.25	1.3973	1.3571	1.4661	0.0183

MULTIPOLE EFFECTS AND FIELD QUALITY

The magnet field quality can be characterized by the higher-order multipoles. We define the relative multipole coefficient as $B_{n+1}^{(m)} = b_n/b_m$, where $b_n = \frac{1}{n!}\frac{\partial^n B_y}{\partial x^n} r^n$ is the $2(n+1)$-pole field strength at radius r. $m = 1, 2$ for the main quadrupole and sextupole field, respectively.

To understand the effect of the multipole errors on the beam dynamics, we take the 20-pole systematic component as an example. The Hamiltonian can be written as: $H_{10} = -\frac{1}{B\rho}\frac{1}{10!}\frac{\partial^9 B_y}{\partial x^9}(x^{10} - 45x^8y^2 + \cdots)$, where $B\rho$ is the rigidity of the beam, B_y is the vertical component of the magnetic field, and $x = x_{c.o.} + x_\beta$, where $x_{c.o.}$ denotes the horizontal closed orbit, and $x_\beta = \sqrt{2\beta_x J_x} cos\psi$ is the betatron oscillation amplitude. Because $x \gg y$, the Hamiltonian is dominated by the first term. And the tune change due to this term is $\nu_{10} = \frac{1}{2\pi}\frac{\partial}{\partial J_x}\langle H_{10}\rangle = -\frac{1}{2\pi}\frac{1}{B\rho}\frac{1}{10!}\frac{\partial^9 B_y}{\partial x^9} \times \sum_{k=1}^{5} kC_{10}^{2k} x_{c.o.}^{10-2k} (2\beta_x)^k \langle \cos^{2k}\psi\rangle J_x^{k-1}$.

Therefore the detuning effect is related to the powers of the closed orbit $x_{c.o.}$ and the horizontal beta function β_x. Bearing in mind that $x_{c.o.}$ is related to dispersion, one can conclude that higher-order multipoles at large dispersion would introduce large momentum dependence of the horizontal tune-shift with amplitude.

Fig. 4 shows the off-momentum β_x and $x_{c.o.}$ for a typical DBA cell. We notice that the closed orbit offset for the off-momentum particles reaches a maximum at the center of the DBA due to linear dispersion. The absolute displacement is much bigger at $\delta = -2.5\%$ than at $\delta = 2.5\%$. This is mostly due to the second-order dispersion being nega-

tive. The beta function for $\delta = -2.5\%$ is also bigger than it is for the on-momentum and positive momentum particles at the center of the arc. With greater closed orbit and beta function, we expect the detuning effect is larger at negative momentum.

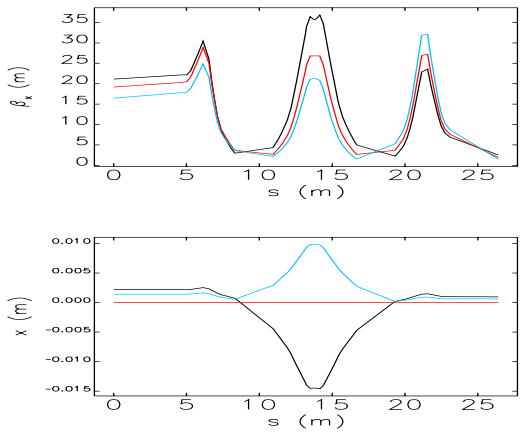

Figure 4: β_x and $x_{c.o.}$ for a DBA cell at $\delta = -2.5$ (black),0 (red) ,2.5% (blue).

Based on the understanding of the multipole effects, we decided to give tighter specifications for the magnets at maximum dispersion. The apertures for the normal quadrupole and sextupole magnets are 66 and 68 mm, respectively. The magnets at the maximum dispersion are designed to have apertures of 90 and 76 mm, respectively. Tab. 3 lists the specifications for the symmetry-allowed multipoles. The unallowed multipoles are in general smaller than the allowed terms. For a complete list of the harmonics one can refer to the NSLS-II design documents [1].

Table 3: The specifications for the allowed multipoles. Units: $\times 10^{-4}$, reference radius r=25 mm.

Quad.	66mm	90 mm	Sext.	68 mm	76 mm
B6	1	0.5	B9	1.0	0.5
B10	3	0.5	B15	0.5	0.5
B14	2	0.1	B21	0.5	0.5

Fig. 5 shows tune versus oscillation amplitude for the lattice at $\delta = -2.5\%$ with ideal magnets (black) and with field errors (red). The difference is apparent. The dynamic aperture is directly affected by this change. The particle motion is stable, until the tune reaches a resonance line as it varies with the oscillating amplitude. At $\delta = -2.5\%$ the dynamic aperture is partly bounded by the resonance line $9\nu_x = 300$. In Fig. 5, one sees that the tune reaches the resonance line at much smaller amplitude when the errors are included. This detuning effect is less at $\delta = 0$ and 2.5%. Fig. 6 is a comparison of the frequency maps with ideal magnets and with the specified multipole errors. The dynamic aperture at negative momentum is smaller with

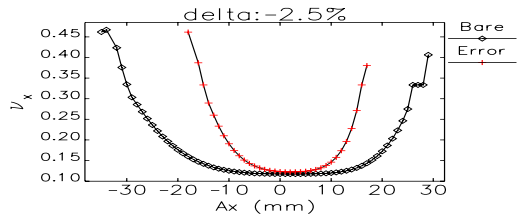

Figure 5: The ring tune changes with amplitude at $\delta = -2.5\%$. Black diamonds: lattice with ideal magnets; red crosses: lattice with enlarged multipole errors.

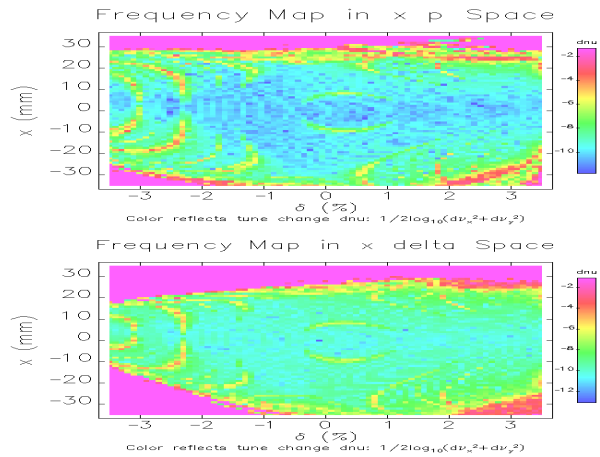

Figure 6: Frequency map comparison between the lattices with ideal magnets (upper plot) and with systematic field errors from Tab. 3 (lower plot).

errors, but it is still adequate for the required 2.5% momentum aperture.

SUMMARY

We have presented the physics considerations for the NSLS-II magnets. The quadrupole tuning range is deduced from the variation of working point and beta functions in the straights. The magnetic multipoles increase the amplitude tune dependence prominent at negative momentum. For NSLS-II tighter multipole specifications were given for the magnets at the maximum dispersion.

REFERENCES

[1] NSLS-II Conceptual Design Report,http://www.bnl.gov/nsls2/project/CDR/